



Cleaning of Filter Cartridges with Convergent Trapezoidal Pleat Shape via Reverse Multi-Pulsing Jet Flow

Shaowen Chen^{1*}, Da-Ren Chen²

¹ School of Energy Science and Engineering, Harbin Institute of Technology, Harbin, Heilongjiang 150001, China

² Particle Lab, Department of Mechanical and Nuclear Engineering, Virginia Commonwealth University, Richmond, VA 23294, USA

ABSTRACT

Pleat structure and tight pleat spacing of pleated filter cartridges often lead to patchy cleaning when applying reverse pulsing technique process to regenerate filter media, consequently resulted in the decrease of the efficiency and quality of reverse pulsed-jet cleaning as well as the service lifetime of filtration units. For improving the non-uniform cleaning or patchy cleaning, a novel convergent trapezoidal pleat shape was used in multi-pulsing reverse flow cleaning. A transient 3D CFD simulation in a simple filtration system with a single filter cartridge was carried out under the four multi-pulsing modes. The effects of multi-pulsing flow cleaning on the cleaning efficiency and quality were systematically investigated. Compared with single-pulsing cleaning mode, the peak pressure differences at the upper regions all became positive because of the increased cleaning frequency, and thus which would be crucially important for improving the local cleaning mechanical stresses and cleaning efficiency. Moreover, the extra peak-pressure augment in the lower regions of filter cartridge also had a positive influence of local cleaning efficiency. For the multi-pulsing scheme of Waveform #4, the peak pressure difference at the section 4 increased by 11.2% than the single-pulsing scheme. The related action mechanism had high correlation with the interaction of residue gas and following jet. Finally, the improvement of the cleaning efficiency and quality are expected to be validated under the decreasing tank pressure and real permeability.

Keywords: Pleated filter cartridge; Reverse multi-pulsing cleaning; Cleaning efficiency; Cleaning quality; Convergent trapezoidal pleat shape.

INTRODUCTION

Reverse pulsing jet cleaning has been widely adopted in industrial filtration applications for periodical regeneration of cartridge filter media (Leith and Ellenbecker, 1980; Lu and Tsai, 1996; Itoa *et al.*, 1998; Simon *et al.*, 2007). In continuous filtration systems either for powder material recovery or particulate matter removal, reverse pulsing jet cleaning is considered as the standard technique to maintain economical filtration operation. Compared with baghouse filters, pleated cartridge filters provide special advantage in enabling a large filtration area being arranged in a compact container and in having low pressure drop in the filtration operation (Chen and Pui, 1996; Wakeman *et al.*, 2005). The pleat structure and tight pleat spacing of filter cartridges often lead to patchy cleaning, thus decreasing the cleaning efficiency and quality, and the service lifetime of filtration

units. The patchy cleaning means the non-uniform cleaning reflected in various modes, including the temporal and spatial non-uniformity. In addition, lowering cleaning energy and air tank pressure are much desired in the advanced design of pleated filter cartridges.

For cartridges with classical V-shaped pleats the media pleating parameters (i.e., pleat pitch, height and count as well as filter properties) and the operational variables of reverse pulsing jet (i.e., the air tank pressure, and pulse timing and duration) have their individual effects on the cleaning performance of a pleated cartridge. The research of reverse pulsing jet cleaning has been focused on the improvement of cleaning efficiency and quality for pleated filter cartridges by varying operational and pleating parameters (Calle *et al.*, 2002; Lo *et al.*, 2010a; Lo *et al.*, 2010b; Bemer *et al.*, 2013; Yan *et al.*, 2013; Qian *et al.*, 2014; Li *et al.*, 2015a; Li *et al.*, 2015b; Yan *et al.*, 2015). The performance of pleated filter cartridges (with different pleat geometries and filter medium properties) under various cleaning conditions (i.e., cleaning mode and tank intensity) was investigated in a full-sized dust collector periodically cleaned by a reverse pulsing jet (Lo *et al.*, 2010a). It was found that the pleat ratio (the ratio of pleat height to pleat pitch) had great

* Corresponding author.

Tel.: 86-138-4504-4501; Fax: 86-451-8641-2017
E-mail address: cswemail@hit.edu.cn

influence on the cleaning efficiency of pleated cartridges and the tank pressure is critical for the pulsing jet cleaning. More, the cleaning quality is varied with the change of cleaning modes. The ineffective cleaning was shown for reverse pulsing jet cleaning in certain cleaning modes (Calle *et al.*, 2002; Bemer *et al.*, 2013). Pre-coating (Bemer *et al.*, 2013) and cone installation (Li *et al.*, 2015a) of pleated filter cartridges have shown to have positive impact on the efficiency and quality of reverse pulsing jet cleaning. The optimization of nozzles (Yan *et al.*, 2013; Qian *et al.*, 2014; Yan *et al.*, 2015) and tank pressure (Lo *et al.*, 2010a; Yan *et al.*, 2015) have also evidenced the reduction of incomplete cleaning or patchy cleaning under certain conditions. However, the poor cleaning quality and patchy cleaning near the head of filter cartridges remains an issue for reverse pulsing jet cleaning.

With the increase of computer power and memory, the modeling of filtration systems under the process of reverse pulsing jet cleaning becomes feasible on workstations. The calculation of pressure and flow fields around pleated cartridges has been performed to evaluate the efficiency of reverse pulsed-jet cleaning (Ahmadi and Smith, 2002; Lo *et al.*, 2010a). Time-dependent 3D models were developed to explore the relationship between cleaning efficiency and filter pleating parameters. The average static pressure and static pressure distribution on the surface of cartridge filter media, which is difficult to be measured, were concluded as the good indicator for cleaning filter cartridges (Lo *et al.*, 2010a). Numerical modeling of time-dependent gas flow field and pressure distribution in pulsing-jet cleaning of baghouse filters was also performed (Ahmadi and Smith, 2002). Satisfactory result on the performance of reverse pulsing-jet cleaning for baghouse filters and pleated filter cartridges were achieved via the numerical modeling.

In this study we investigated the cleaning of filter cartridges with convergent trapezoidal pleats via reverse multi-pulsing jet flow. The filter cartridges with convergent trapezoidal pleats offer the better solution to efficiently increase the static pressure drop across pleated filter media. It has been evidenced in our previous works (Chen and Chen, 2016; Chen *et al.*, 2017) filter cartridges equipped with convergent trapezoidal pleats offer improved efficiency and quality when they are cleaned by reverse pulsing jet flow. In the meantime, the patchy cleaning issue encountered in the case of filter cartridges with classical V-shaped pleats can be minimized using reverse multi-pulsing jet flow. We thus hypothesized that the combination of both should offer even better cleaning efficiency and quality for pleated filter cartridges. We proposed to clean filter cartridges via multiple pulsing jets, instead of one single pulsing typically applied in existed filtration systems (under the assumption of the same total duration for tank valve opening). This reverse cleaning method is called as the “reverse multi-pulsing jet cleaning” way. The effect of multi-pulsing schemes on the cleaning efficiency and quality for studied filter cartridges was studied via a transient 3D CFD modeling of a simple filtration system having a single filter cartridge. Numerical modeling was thus performed for this investigation and the result of our investigation is presented in the following.

NUMERICAL MODEL AND METHODS

Numerical Model

Shown in Fig. 1 is the studied filter cartridge with convergent trapezoidal pleats which have larger spacing at the pleat tips compared with that of typical V-shaped pleats. The thickness of filter media is assumed 0.8 mm and the total pleat count is 40. The choices of 0.8 mm medium thickness and 40 pleat counts are based on the literatures (Lo, 2006; Lo *et al.*, 2010a). The other schemes with different filter mediums and pleat counts have not been studied in the research so far. As seen in Fig. 1, the width of top surface of the filter pleat with a convergent trapezoidal shape is defined as “W”, and the “C” represents the pleat pitch. The schematic diagram of the single-unit filtration system under this study is also shown in Fig. 2. The injection nozzle (with the ID of 5 mm) was placed along the axis of filter cartridges. Because of the axisymmetric arrangement of the studied system, a single pleat was modeled

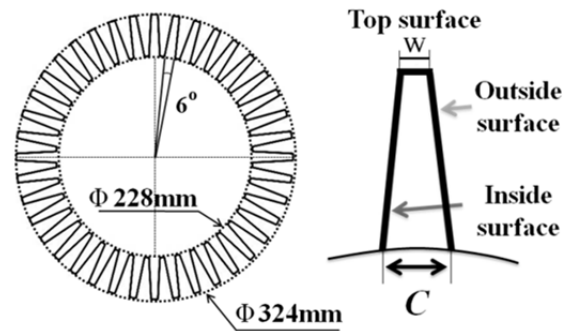


Fig. 1. Schematic diagram of studied filter cartridges with convergent trapezoidal pleats.

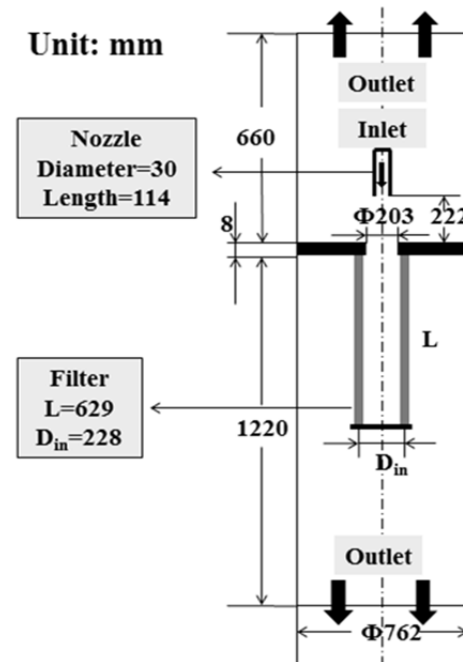


Fig. 2. Diagram of a studied filtration system with single filter cartridge in this study.

in our study. In reality, once the cleaning is initiated, high pressure gas flows through a solenoid valve, a long flow tube and reach injection nozzle from a pressure tank. Since the flow in the gas delivery pipelines is not the focus of this study, the gas flow rate exited from the nozzle was modeled by assuming a given time-dependent total pressure at the nozzle inlet.

Four different pulsing modes (i.e., waveforms) for the transient total pressure at the nozzle inlet (shown in Fig. 3(a)) were investigated. They include the single pulsing mode (i.e., Waveform #1, representing the mode in standard industrial filtration systems) and three other hypothetical total pressure modes (i.e., Waveforms #2, #3 and #4, respecting the multiple pulsing modes). The design of these waveforms was based on the data given in the work of Lo

(2006): when the tank pressure and pulse duration were set at 482,370 Pa and 0.35 s, respectively, the highest total pressure and pulse duration measured at the nozzle inlet were 45,000 Pa and 0.5 s during air injection, respectively. For comparison the peak total pressure and total pulse duration in all the modes were kept identical. The case of Waveform #1 mode operation was used as the reference.

Standard atmospheric pressure was applied as an average static pressure at the outlets of computational domain. The inlet static temperature and turbulence intensity was assumed to be 300 K and 5%, respectively.

Numerical Methods

The CFD ANSYS CFX R.14 code (ANSYS, 2011) was used to calculate the flow and pressure fields in the studied

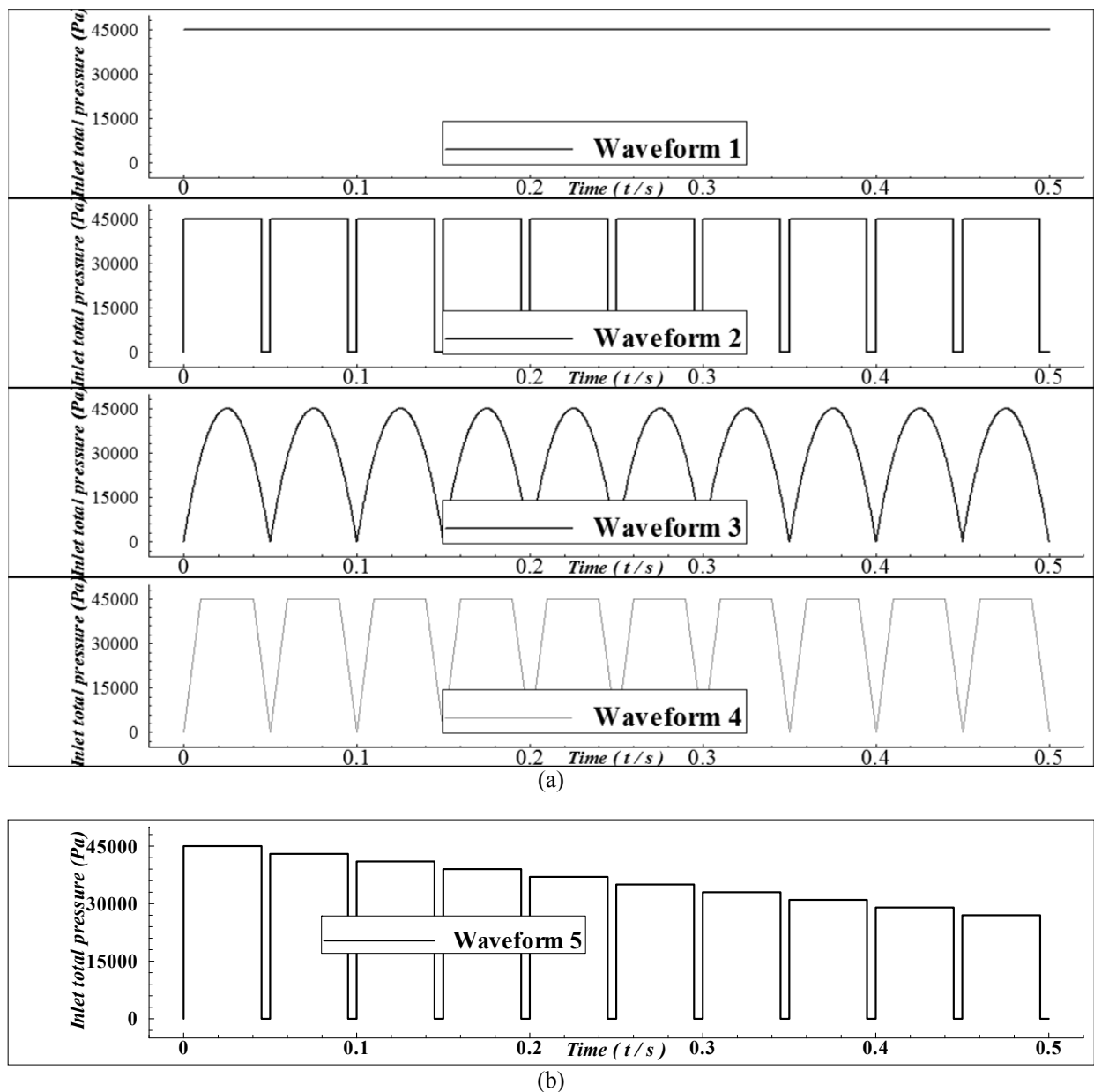


Fig. 3. Schematic diagram of studied reverse flow pulsing schemes (a) with constant peak inlet pressure; (b) with the consideration of peak inlet pressure reduction due to the depletion of gas tank during a cleaning cycle.

filtration system under the reverse pulsing-flow cleaning. Unsteady Reynolds-averaged Navier-Stokes equations were solved. The step for matching in time was 0.0003 s. The second-order backward Euler scheme was applied to the transition terms in the governing equations. The flow in the porous media was assumed isothermal and the total energy was set in the fluid domain. The SST $k-\omega$ turbulent model with second-order accuracy was applied as the wall function. The above modelling has been extensively validated for a wide range of flows (Menter *et al.*, 2003).

Structured meshes were generated using the commercial software of mesh generation, ANSYS ICEM CFD R.14. Structured meshes with three-dimensional hexahedral elements were selected in this modeling. Meshes nearby the surface of filter media and nozzle were refined to ensure the y^+ (y^+ : dimensionless wall distance) of the first mesh layer near the surfaces is less than 1.0. Fig. 4 shows a typical computational domain used in the study. The number of mesh nodes used in the computational domain was 1.3 M with encrypted meshes on the surface of filter media (approximate 0.1 M).

Total-pressure boundary conditions were set at the inlet and outlet of the computational domain. The transient distribution of total pressure at the inlet was given in Fig. 3 and the back pressure at the outlet was a standard atmospheric pressure, set as average static pressure over the entire outlet. The computational domain consisted of three subdomains - two for fluid and one for porous domain. Domains with different physical parameters were connected via GGI (General Grid Interface), allowing the total energy to flow through the fluid-porous interface.

Flow in porous media can be calculated in the CFX (ANSYS, 2011) using the model for momentum loss (or full porous medium model). An isotropic porous filter media was assumed. K_1 and K_2 are the permeability and quadratic

loss coefficient, respectively. In this study, K_1 and K_2 were set to $2 \times 10^{-12} \text{ m}^2$ and $1,000 \text{ m}^{-1}$, respectively, obtained from the filter-testing data reported in the work (Lo, 2006). The filter porosity of 0.99 was given for filter media. The deformation of filter media during the pulsing-jet cleaning was not considered in this modeling.

RESULTS AND DISCUSSION

It has been observed that the top section of filter cartridges have the worst cleaning efficiency and quality under the reverse single pulsing jet flow cleaning in the literatures (Lo *et al.*, 2010b; Yan *et al.*, 2013). To improve the non-uniform cleaning at the top section of filter cartridges, we had proposed a novel cleaning technique utilizing multiple pulsing jet flow in one cleaning cycle (Chen and Chen, 2016). The concept of multiple pulsing jet flow for cleaning is derived from the observation that, in a single pulsing jet cleaning process, the cleaning action at the cartridge top becomes very ineffective when high-speed flow jet flow reaches the cartridge base (because of the presence of low positive or even negative static pressure). High positive static pressure at the cartridge top only happens once in a very short time when the jet stream flows through the filter media at the top cartridge section. The multiple pulsing jet flow for cleaning was thus suggested to increase the number of cleaning counts at the cartridge top session.

Peak Static Pressure Difference

Static pressure difference is a good indicator for the efficiency and quality of reverse pulsing jet flow cleaning. The static pressure difference discussed herein is defined as the area-averaged static pressure difference between the inner and outer surfaces of filter media packed in cartridges. The higher static pressure difference results in the higher mechanical stresses for cleaning. The static pressure difference was used as a better indicator for the efficiency and quality of reverse pulsing jet flow cleaning in our previous works (Chen and Chen, 2016; Chen *et al.*, 2017). Fig. 5 shows the distribution of peak static pressure difference at different sections of studied filter cartridge at $t = 0.2 \text{ s}$ to 0.3 s . Note that, for later data analysis, studied filter cartridge was evenly divided into ten sections from the base to the top of the filter cartridge (numbered from Area 1 to 10 accordingly) as shown in the right of Fig. 5. For all three multi-pulsing modes, the peak pressure difference at the cartridge top and base was all increased except for the cartridge sections numbered 6 in the case of the Waveform #3 scheme. In this exceptional case the changing of pressure difference was more gradual than that using the single-pulsing mode (i.e., Waveform #1). Compared with the single pulsing jet cleaning, the peak static pressure difference at the top cartridge sections (i.e., Area 7–10) apparently increased and had undergone the significant transition of surface pressure difference from the negative value to positive. The above pressure difference transition is expected to result in the local cleaning mechanical stresses on filter surface, improving the cleaning efficiency and quality. The increase of static pressure difference at the cartridge base sections

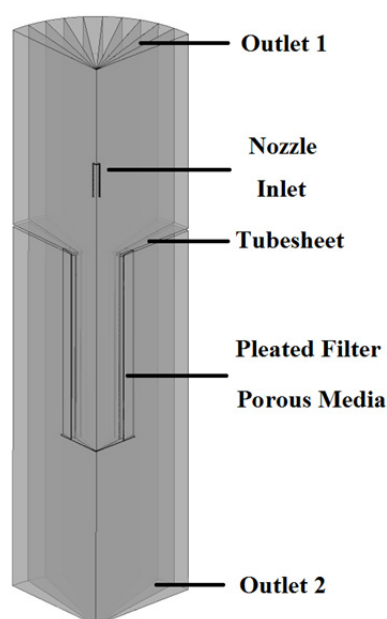


Fig. 4. Schematic diagram of a typical computational domain (10 copies, 1/4 circle).

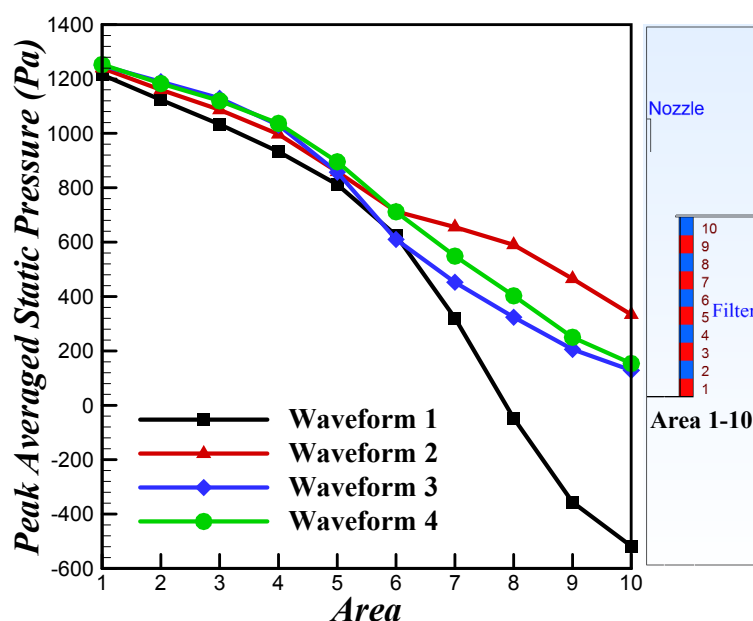


Fig. 5. Distribution of average peak pulse pressure at various sections of studied filter cartridges ($t = 0.2\text{--}0.3$ s). Note that the base section of studied cartridge was labeled as Area 1 and the top section as Area 10.

(i.e., Area 1–5) was smaller than that at the top sections. Nonetheless, slightly increased peak-pressure difference will have positive impact on the cleaning efficiency.

Table 1 gives the percentage of increased peak pressure difference at various base sections of studied cartridge during $t = 0.2\text{--}0.3$ s. The peak pressure difference in the case of Waveform #1 was used as the reference. For all three studied multi-pulsing schemes, the maximal enhancement occurred at the section 4, i.e., 6.9% for Waveform #2, 10.5% for Waveform #3 and 11.2% for Waveform #4.

Transient Averaged Static Pressure

In some previous studies (Simon *et al.*, 2007; Lo *et al.*, 2010a; Yan *et al.*, 2015), the time-dependent static pressure were chosen as the indicator for efficiency and quality of reverse flow cleaning (instead of peak pressure difference). Fig. 6 thus provides a time-dependent averaged static pressure at various cartridge sections. In the case of Waveform #1 (typical single-pulsing cleaning) the high pressure fluctuations at the sections of Area 8–10 briefly occurred in the initial cleaning phase. The static pressure was then gradually reduced and approached to a negative value after approximate 0.01 s. The static pressure on the top cartridge sections was negative for a very brief period of time, which was one of primary reasons for the observed patchy cleaning. However, in the cases of multi-pulsing cleaning, the high pressure fluctuation at the top cartridge sections occur frequently according the pulsing frequency, resulting in the positive pressure repeatedly forced on the filter surface. For multiple pulsing jet cases, the static pressure on the surface of base cartridge sections (Area 1–3) had distinguished characteristics for each pulsing jet after the 1st one. The multi-pulsing cleaning does reduce the average static pressure in a short period time (i.e., the transition between two pulsing). There is no evidence indicating that low static pressure would

Table 1. The enhancement of average peak pressure at the base sections of studied filter cartridges ($t = 0.2\text{--}0.3$ s) (The “ P_{a1} ”, “ P_{a2} ”, “ P_{a3} ”, “ P_{a4} ” and “ P_{a5} ” represent the peak static pressure difference at the Area 1, 2, 3, 4 and 5, respectively).

Increasing rate (%)	P_{a1}	P_{a2}	P_{a3}	P_{a4}	P_{a5}
Waveform 2	2.0	3.3	5.1	6.9	5.8
Waveform 3	2.7	5.9	9.3	10.5	5.6
Waveform 4	3.1	5.3	8.3	11.2	10.3

decrease the cleaning efficiency and quality for filter cartridges (as long as the critical static pressure is achieved). Consequently, the transient reduction in the average static pressure was thought not to have a negative effect on the cleaning efficiency and quality.

Further, the rapid variation of mechanical forces resulted from the large static pressure change could lead to a sudden acceleration of filter media near the cartridge top sections, consequently facilitating dust cake detachment from filter surface (Simon *et al.*, 2007). As evidenced in Fig. 6, the cleaning scheme of Waveform #2 would provide the rapidest static pressure increase at the top cartridge sections compared with that in other two multi-pulsing waveforms.

Static Pressure and Velocity Distributions

As observed in Fig. 6 the characteristics of average static pressure evolution during the first pulsing period of time is obviously different from those in the sequential pulsing. Fig. 7 shows the comparison of the transient distribution of static pressure for the pulsing mode with Waveform #2 at two time instances ($t = 0.003$ s and 0.153 s). At these two instances initiated jet flows just entered the studied filter cartridge. The static pressure in the cartridge at $t = 0.153$ s is clearly higher than that at $t = 0.003$ s while the static

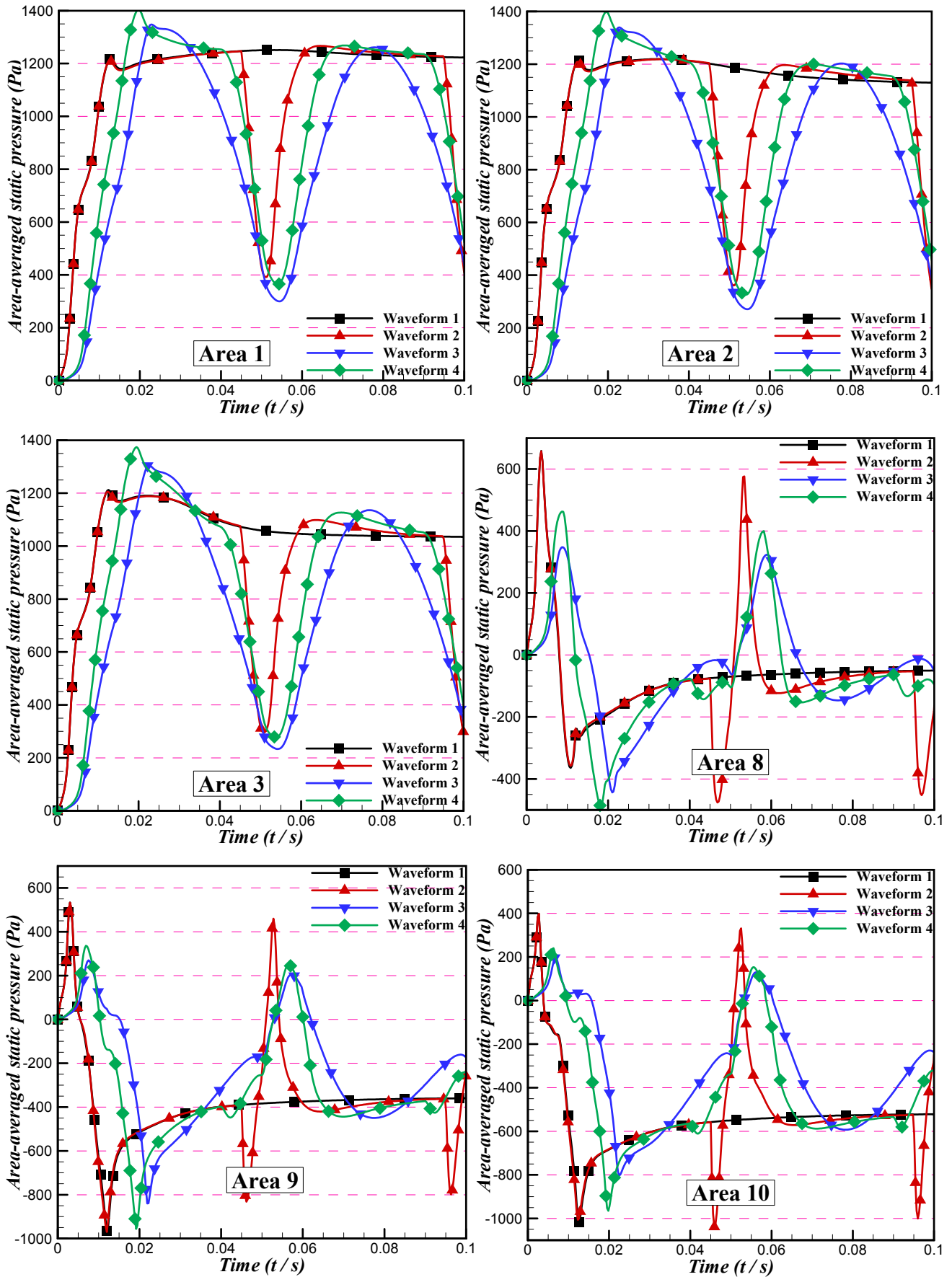


Fig. 6. Time-dependent area-averaged static pressure at selected sections of studied filter cartridges ($t = 0\text{--}0.1$ s)

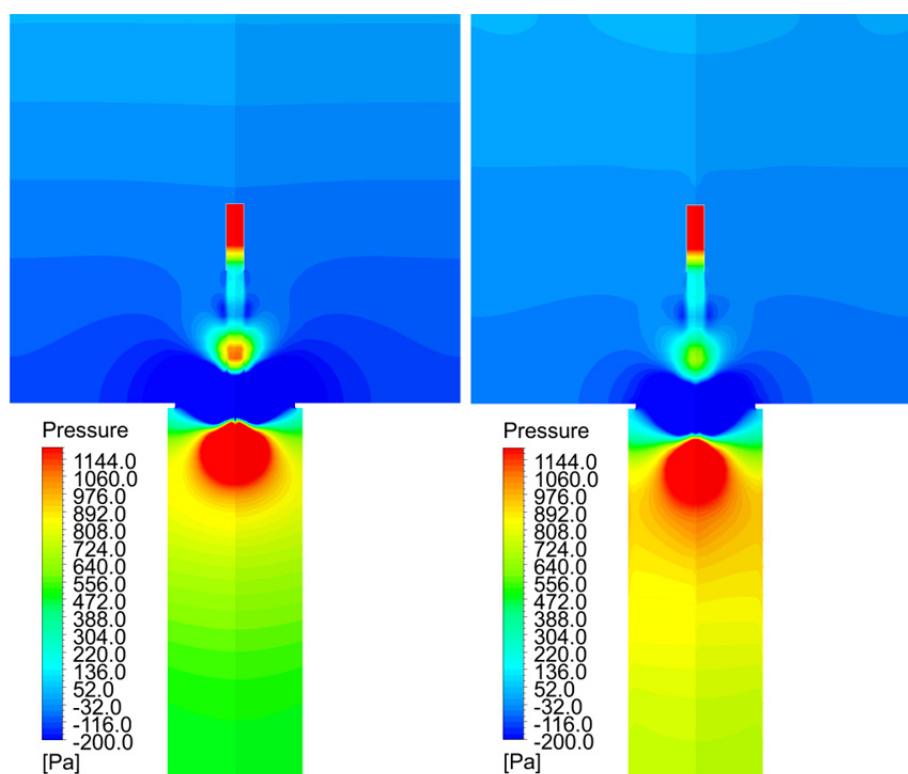


Fig. 7. Comparison of transient static-pressure distribution at two selected time instances in the case with the pulsing scheme of Waveform 2: (a) the 1st pulse jet, $t = 0.003$ s; (b) the 4th pulse jet, $t = 0.153$ s.

pressure near the nozzle outlet at $t = 0.153$ s is lower than that at $t = 0.003$ s. Towards the ending of each flow pulsing, high-pressure residual gas in the cartridge had no sufficient time to be completely released. High-pressure was thus established in the cartridge because of the interaction of residue gas and pulsing jet. The increase of peak pressure at the cartridge base is also highly correlated with above-identified flow interaction.

Effects of Gas Tank Pressure Decrease

In the practical cleaning operation, the compressed gas tank pressure is decreased with time because of finite mass of gas stored in the tank and insufficient time to fill it up during the reverse flow cleaning. The tank pressure reduction during the cleaning leads to the drop in pulse-jet pressure, consequently affecting the cleaning efficiency. To investigate the effect of total tank pressure reduction in each cleaning cycle, we used the waveform #5 (shown in Fig. 3(b)) to model the nozzle inlet pressure. With the decrease of total inlet pressure, as shown in Fig. 8, the average peak pressure at the cartridge base was reduced gradually according to the modeled reduction trend of total inlet pressure, indicating the potential decline of local cleaning efficiency and quality for reverse multi-pulsing cleaning. The reduction of average positive peak pressure at the cartridge top was apparently slower than that at the cartridge base. Additionally, the average negative peak pressure at the filter top was increased. It is thus concluded that the decrease of total tank pressure may result in the decrease of cleaning efficiency and quality for multi-pulsing cleaning. The similar trend

was observed in the case for a single-pulsing scheme.

Effect of Dust Cake Removal during the Cleaning Cycle

We consider the cartridge filter media and built-up dust cake as one single layer of porous media with a time-dependent permeability to model the effect of dust cake removal on the cleaning efficiency of reverse pulsing flow process. According to the study of dust cake release behavior as a function of time (Ferer and Smith, 1997), the time-dependent permeability during the cleaning was assumed to follow a logarithmic cake release mode (shown in Fig. 9). Based on the measured data of Al_2O_3 particles given in the literature (Lo, 2006), the initial permeability of filter media with dense dust cake was $3.03692 \times 10^{-14} \text{ m}^2$ and final permeability of filter media with loose dust cake was 3.5×10^{-12} . Fig. 10 shows the comparison of average static pressure for studied filter cartridges under the reverse pulsing flow cleaning with the Waveforms #1 and #2. In general the pressure variation and distribution had similar characteristics with in the cases without dust cake. The improvement of efficiency and quality for cleaning studied filter cartridges was validated even in the cases considering the removal of built-up dust cake during the reverse multi-pulsing jet. In particular, the higher peak pressure in the first pulsing jet when the media permeability was low was observed when compared to that in the case without the consideration of dust cake removal. For the base sections of filter cartridge the peak pressure in each pulsing process of Waveform #2 was decreased with the increase of permeability during the dust cake removal.

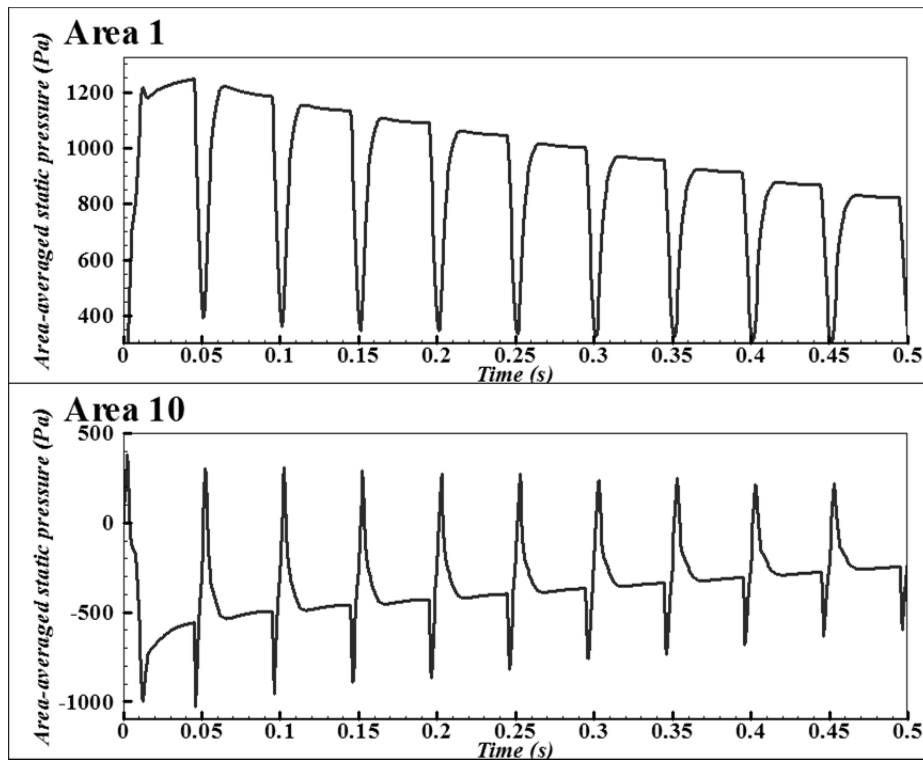


Fig. 8. Distribution of time-dependent area-averaged static pressure at the base and top regions of studied filter cartridges under the condition considering the decrease of gas tank pressure during a cleaning cycle ($t = 0\text{--}0.5$ s).

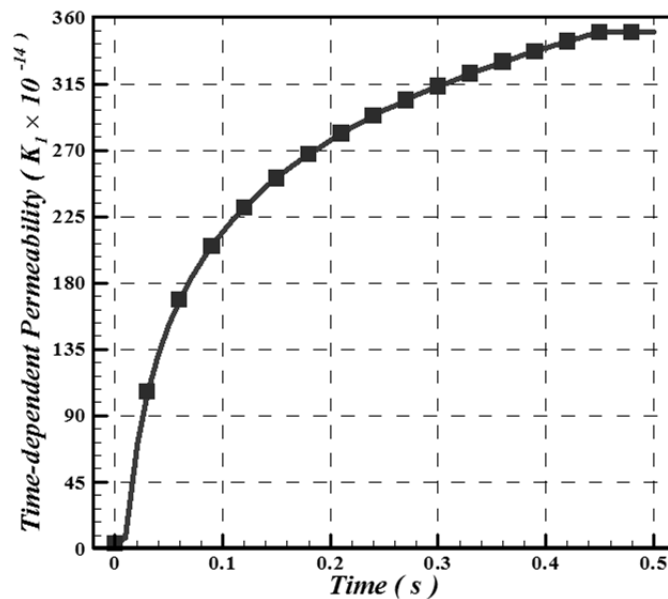


Fig. 9. Assumed transient permeability of media undergoing the dust cake removal in a cleaning cycle pulse

CONCLUSION

With the ultimate goal of finding efficient solutions to solve the patchy cleaning issue of reverse flow technique, we investigated the cases of filter cartridges having convergent trapezoidal pleats undergoing a reverse multi-pulsing jet cleaning process.

For the case with the standard single-pulsing scheme, the

top sections of studied cartridge under the condition of negative pressure difference was approximately one-third of entire filter cartridges. By applying the multi-pulsing cleaning schemes, the peak pressure difference at the top cartridge sections became positive (because of the increased pulsing frequency). The pressure change at the top sections of filter cartridges is of importance to increase the local cleaning mechanical stress and improving the local cleaning

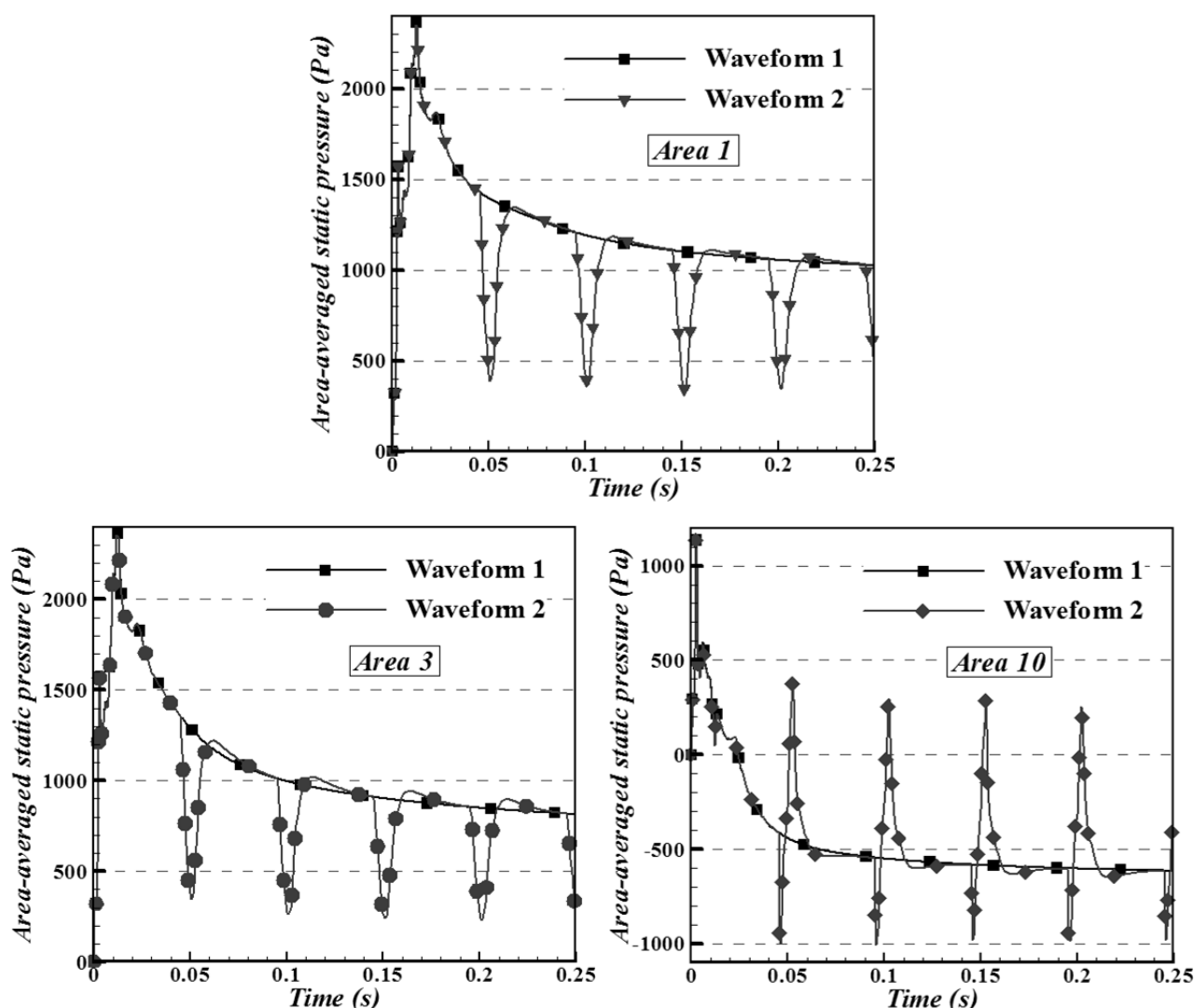


Fig. 10. Comparison of area-averaged static pressure difference as a function of time when applying the pulsing schemes of Waveform #1 and #2 and with the consideration of dust cake removal ($t = 0\text{--}0.25$ s)

efficiency. Similar pressure enhancement was observed at the base sections of studied cartridges even though the enhancement was less than that at the top sections. The additional peak-pressure increase at the base sections of cartridges is also expected to have positive influence on local cleaning efficiency. For all three studied multi-pulsing schemes, the maximal augment occurred at the section 4, i.e., 6.9% for Waveform #2, 10.5% for Waveform #3 and 11.2% for Waveform #4. The related action mechanism was highly correlated with the interaction of residual gas in cartridges from a former pulsing jet and later jet.

The effects of gas tank pressure decrease (due to finite mass stored in the tank) and permeability change (due to the dust cake removal) on the cleaning efficiency and quality for filter cartridges with convergent trapezoidal pleats were further investigated. The positive effect to improve the cleaning efficiency and quality by reverse multi-pulsing flow was confirmed for studied cartridges. The decrease of total tank pressure may result in the decrease of cleaning efficiency and quality for multi-pulsing cleaning.

ACKNOWLEDGEMENTS

The authors are grateful to the support of the China Scholarship Council (CSC). The authors would also like to acknowledge the suggestion and assistance of Dr. Qiang Wang of Virginia Commonwealth University.

REFERENCES

- Ahmadi, G. and Smith, D.H. (2002). Analysis of steady-state filtration and backpulse process in a hot-gas filter vessel. *Aerosol Sci. Technol.* 36: 665–677.
- Bemer, D., Regnier, R., Morele, Y., Gripari, F., Appertcollin, J. and Thomas, D. (2013). Study of clogging and cleaning cycles of a pleated cartridge filter used in a thermal spraying process to filter ultrafine particles. *Powder Technol.* 234: 1–6.
- Calle, S., Contal, P., Thomas, D., Bemer, D. and Leclerc, D. (2002). Evolutions of efficiency and pressure drop of filter media during clogging and cleaning cycles.

- Powder Technol.* 128: 213–217.
- Chen, D. and Pui, D.Y.H. (1996). Optimization of pleated filter designs. *J. Aerosol Sci.* 27: 654–655.
- Chen, S. and Chen, D. (2016). Numerical study of reverse multi-Pulsing jet cleaning for pleated cartridge filters. *Aerosol Air Qual. Res.* 16: 1991–2002.
- Chen, S., Wang, Q. and Chen, D. (2017). Effect of pleat shape on reverse pulsed-jet cleaning of filter cartridges. *Powder Technol.* 305: 1–11.
- Ferer, M. and Smith, D.H. (1997). A simple model of the adhesive failure of a layer: cohesive effects. *J. Appl. Phys.* 81: 1737–1744.
- Itoa, S., Tanakaa, T. and Kawamurab, S. (1998). Changes in pressure loss and face velocity of ceramic candle filters caused by reverse cleaning in hot coal gas filtration. *Powder Technol.* 100: 32–40.
- Leith, D. and Ellenbecker, M.J. (1980). Theory for pressure drop in a pulse-jet cleaned fabric filter. *Atmos. Environ.* 14: 845–852.
- Li, J., Li, S. and Zhou, F. (2015a). Effect of cone installation in a pleated filter cartridge during pulse-jet cleaning. *Powder Technol.* 284: 245–252.
- Li, Q., Zhang, M., Qian, Y., Geng, F., Song, J. and Chen, H. (2015b). The relationship between peak pressure and residual dust of a pulse-jet cartridge filter. *Powder Technol.* 283: 302–307.
- Lo, L. (2006). *Experimental Study and Numerical Analysis for Pleated Filter Cartridges in a Pulse-Jet Cleaned Dust Collector*. Ph. D. Thesis, University of Minnesota, Twin Cities.
- Lo, L., Hu, S., Chen, D. and Pui, D.Y.H. (2010a). Numerical study of pleated fabric cartridges during pulse-jet cleaning. *Powder Technol.* 198: 75–81.
- Lo, L., Chen, D. and Pui, D.Y.H. (2010b). Experimental study of pleated fabric cartridges in a pulse-jet cleaned dust collector. *Powder Technol.* 197: 141–149.
- Lu, H.C. and Tsai C.J. (1996). Numerical and experimental study of cleaning process of a pulse jet fabric filtration system. *Environ. Sci. Technol.* 30: 3243–3249.
- Menter, F.R., Kuntz, M. and Langtry, R. (2003). Ten years of industrial experience with the SST turbulence model. In *Turbulence, Heat and Mass Transfer 4*, Hanjalic, K., Nagano, Y. and Tummers, M. (Eds.), Begell House, New York, pp. 625–632.
- Qian, Y., Bi, Y., Zhang, Q. and Chen, H. (2014). The optimized relationship between jet distance and nozzle diameter of a pulse-jet cartridge filter. *Powder Technol.* 266: 191–195.
- Simon, X., Chazelet, S., Thomas, D., Bemer, D. and Regnier, R. (2007). Experimental study of pulse-jet cleaning of bag filters supported by rigid rings. *Powder Technol.* 172: 67–81.
- Wakeman, R.J., Hanspal, N.S., Waghode, A.N. and Nassehi, V. (2005). Analysis of pleat crowding and medium compression in pleated cartridge filters. *Chem. Eng. Res. Des.* 83: 1246–1255.
- Yan, C., Liu, G. and Chen, H. (2013). Effect of induced airflow on the surface static pressure of pleated fabric filter cartridges during pulse jet cleaning. *Powder Technol.* 249: 424–430.
- Yan, C., Zhang, M. and Lin, L. (2015). On-line pulse-jet cleaning of pleated fabric cartridge filters for collecting pesticides. *RSC Adv.* 59: 48086–48093.
- ANSYS Inc. (2011). ANSYS CFX Theory Guide, Release 14.0, Canonsburg, PA.

Received for review, November 22, 2016

Revised, March 11, 2017

Accepted, March 17, 2017